Articles

Role of Helix B Residues in Interfacial Activation of a Bacterial Phosphatidylinositol-Specific Phospholipase C[†]

Su Guo,[‡] Xin Zhang,[‡] Barbara A. Seaton,[§] and Mary F. Roberts*,[‡]

Merkert Chemistry Center, Boston College, Chestnut Hill, Massachusetts 02467, and Boston University School of Medicine, Boston, Massachusetts 02118

ABSTRACT: The *Bacillus thuringiensis* phosphatidylinositol-specific phospholipase C (PI-PLC), an interfacial enzyme associated with prokaryotic infectivity, is activated by binding to zwitterionic surfaces, particularly phosphatidycholine (PC). Two tryptophan residues (Trp47 in the two-turn helix B and Trp242 in a disordered loop) at the rim of the barrel structure are critical for this interaction. The helix B region (Ile43 to Gly48) in wild-type PI-PLC orients the side chains of Ile43 and Trp47 so that they pack together and form a hydrophobic protrusion from the protein surface that likely facilitates initial membrane binding. In previous studies we reported that in the crystal structure of the dimeric W47A/W242A mutant, which is unable to bind to PC, the helix B region has been reorganized by the mutation into an extended loop. Here we report the construction and characterization (catalytic activity, fluorescence, and NMR studies) of a series of PI-PLC mutants targeting helix B residues and surrounding regions to explore what is needed to stabilize the "membrane-active" conformation of the helix B region. Results strongly suggest that, while hydrophobic groups and presumably an intact helix B are critical for the initial binding of PI-PLC to membranes, disruption of helix B to allow enzyme dimerization is what leads to the activated PI-PLC conformation.

The *Bacillus thuringiensis* phosphatidylinositol-specific phospholipase C (PI-PLC)[1] exhibits a very specific interfacial activation toward monomer and aggregated substrates upon binding to phosphatidylcholine interfaces (*1–3*). Although the $(\beta\alpha)_8$-barrel core of a closely related PI-PLC appears relatively rigid, the crystal structure of the enzyme shows hydrophobic residues at the rim of the barrel in helix B (Ile43–Gly48) and the 237–244 loop with significant mobility as measured by *B* factors (*4*). Previous work has clearly pointed to the importance of Trp47 and Trp242 in binding to activating PC interfaces (and at least one of them crucial for the protein to bind to anionic phospholipid surfaces) (*5–7*). The rim Trp residues have been suggested to be part of a binding site for PC molecules (*8*). Removal of either Trp reduces activation by PC; removal of both renders the enzyme incapable of binding to PC interfaces (*5*). Indeed, for the rim loop interfacial mutants of PI-PLC examined thus

far, the specific activity (in both phosphotransferase and cyclic phosphodiesterase assay systems) correlates with how tightly the PI-PLC binds to activating PC SUVs (Figure 1). However, helix B mutant proteins do not follow this trend. Introduction of a tryptophan at other positions in helix B in the PI-PLC mutant W47A generated proteins that could bind moderately well to PC vesicles. Yet most of those were much less active than wild-type PI-PLC (*7*). Furthermore, the single helix B mutant that regained significant kinetic activation by PC compared to W47A, I43W/W47A, did not bind tightly to PC vesicles (*7*). I43W/W47A has the tryptophan on the same side of the two-turn helix B as Trp47. The lower activity of I43W/W47A as well as the other helix B mutants, which bind PC well but are relatively inactive (*7*), suggests that most of the mutations cannot retain the unusual conformation that is critical for interfacial activity.

Recently, the crystal structure of the *B. thuringiensis* PI-PLC W47A/W242A mutant was solved (*9*). This interfacially impaired PI-PLC is a dimer in contrast to the highly homologous *Bacillus cereus* PI-PLC, which crystallizes as a monomer (*4*). The dimer interface has a hydrophobic core of tyrosine residues that are quite removed from the active site (*9*). In the dimer, residues Ile43 to Gly48 no longer form a helix but instead adopt an irregular loop with an increased distance between residues 43 and 46 (Figure 2). In the *B. cereus* PI-PLC, helix B has the Ile43, Val46, and Trp47 side chains packed together to form a plug extending into solution

[1] Abbreviations: cIP, 1,2-cyclic inositol phosphate; CMC, critical micelle concentration; DAG, diacylglycerol; I-1-P, D-inositol 1-phosphate; iPrOH, 2-propanol; PI, phosphatidylinositol; PI-PLC, phosphatidylinositol-specific phospholipase C; rPI-PLC, recombinant PI-PLC; PC, phosphatidylcholine; POPC, 1-palmitoyl-2-oleoyl-PC; diC₇PC, diheptanoylphosphatidylcholine; SUV, small unilamellar vesicle.
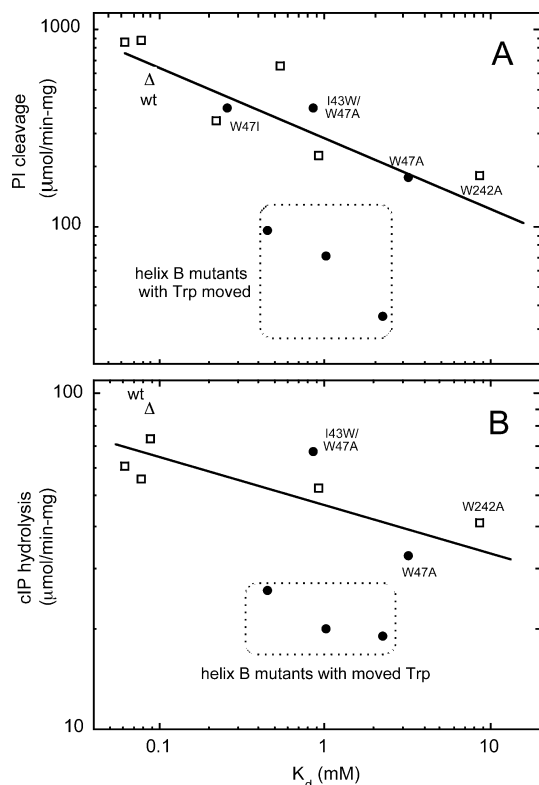
FIGURE 1: Correlation of apparent K_d, which measures the partitioning of PI-PLC and mutants to POPC SUVs, with enzymatic activity toward (A) 8 mM PI solubilized in 24 mM diC$_7$PC or toward (B) 5 mM cIP with 5 mM diC$_7$PC added. Squares represent W242A and rescue mutants, the open triangle is wild-type rPI-PLC, and the filled circles are helix B W47A and rescue mutants (data from ref 7).
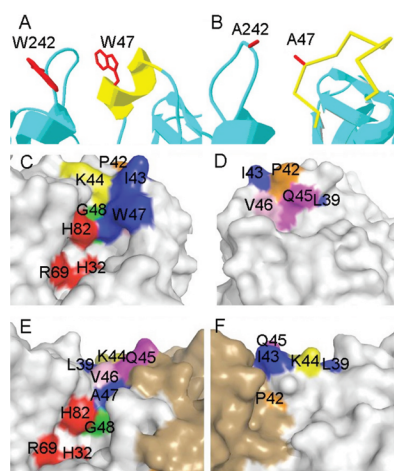

FIGURE 2: Local structure of helix B in (A) *B. cereus* PI-PLC and (B) a monomer of *B. thuringiensis* W47A/W242A PI-PLC. (C–F) Surface representations showing the location of helix B residues (Pro42, orange; Ile43, blue; Lys44, orange; Gln45, magenta; Val46, pink; Trp47, blue; and Gly48, green) and their relation to active site residues (His32, Arg69, and His82 colored in red) in *B. cereus* PI-PLC (C, D) and *B. thuringiensis* W47A/W242A (E, F). For each enzyme the left and right side panels represent "front" and "back" (rotated by 180°) views of the helix B, active site, and dimerization interface regions of the protein.

(4). Such a hydrophobic plug could aid in initiating and stabilizing membrane binding. In the W47A/W242A double mutant, the Ile43 side chain is reoriented toward the protein core (9). If attachment of the plug is a part of the initial binding of the protein to a PC interface, then mutations that

destabilize the helix in solution would be expected to reduce PC affinity and lead to lower PC activation of cIP hydrolysis. However, there are interactions of residues in and around helix B (e.g., Pro42 and Gln45) that appear to stabilize the dimer interface, and these cannot be accommodated with a helical structure for this segment of the protein (9).

Here we report the characterization of a series of PI-PLC mutant proteins with alterations of helix B residues (as well as regions around this structural feature). These were constructed to explore what residues in this region of the protein are needed to stabilize the "membrane-active" conformation of the protein. Alanine mutants at each position in helix B (43–48) as well as Leu39 were constructed and characterized for any changes in secondary structure (CD spectroscopy), PC activation of PI cleavage and cIP hydrolysis, and the ability to bind to PC interfaces (comparing both protein intrinsic fluorescence in the presence of PC vesicles and a vesicle filtration assay). Leu39, a hydrophobic amino acid adjacent to the start of helix B, was altered to an alanine to assess its contribution, if any, to membrane binding. The mutated protein that replaces Lys44, the only charged residue in helix B, with an anionic group (Glu) was also examined. Pro42, the residue immediately before the start of helix B, was also altered to P42G, replacing a conformationally restricted residue with a very flexible one.

All of these mutants except K44A exhibited lower activity for one or both steps of PI hydrolysis. However, there were differences among the mutants that allow us to propose a mechanism for PI-PLC activation by PC and to assess the formation of a membrane-induced dimer as a key step for optimal activity. The results are consistent with (i) formation of helix B in solution to prevent premature dimerization of the protein in solution, (ii) initiation of binding to PC-containing membranes by the hydrophobic helix B "plug", and (iii) disruption of helix B once the protein is anchored in preparation for dimer formation with another membrane-bound PI-PLC to generate the "membrane-activated" form of PI-PLC.

EXPERIMENTAL PROCEDURES

Chemicals. Lipid powders or solutions in organic solvent were purchased from Avanti Polar Lipids, Inc., and used without further purification. These included the long-chain lipids 1-palmitoyl-2-oleoylphosphatidylcholine (POPC) and L-α-phosphatidylinositol (PI) from bovine liver and the synthetic short-chain lipid diheptanoyl-PC (diC$_7$PC). Crude soybean PI from Sigma Chemical Co. was used for the enzymatic generation of cIP by PI-PLC as described previously (1). Tryptone and yeast extract were obtained from Fisher, Inc. Most of the other chemicals, such as 2-propanol (iPrOH), chloroform, ethanol, D$_2$O, Tris, HEPES, glycerol, and Triton X-100, were purchased from Sigma. Q-Sepharose fast-flow anion-exchange resin and phenyl-Sepharose hydrophobic resin were purchased from Amersham Pharmacia Biotech; AG1-X8 (chloride form, 100–200 mesh) was obtained from Bio-Rad Laboratories. All competent cells used in mutagenesis (super blue) and overexpression (BL21 Codonplus) were obtained from Stratagene.

Constructing and Overexpression of PI-PLC Mutants. Single PI-PLC mutants (L39A, P42G, I43A, I43W, K44E, Q45A, V46A, G48A) were constructed from the wild-type

B. thuringiensis PI-PLC gene using QuikChange methodology (*10*) with a site-directed mutagenesis kit from Stratagene. The HPLC purified mutagenic primers were purchased from Operon. Mutated genes were sequenced at Sequegen to confirm the identity of the mutation. Also overexpressed were two mutants constructed and reported previously, K44A (*6*) and W47A/W242A (*5*). Several double mutant proteins (L39A/V46A, I43W/W47I) were made by introducing the second mutation in the gene coding for a single mutant. A plasmid containing the mutant *B. thuringiensis* PI-PLC gene was transformed into *Escherichia coli* BL21-Codonplus (DE3)-RIL cells. Overexpression and purification (via elution from a Q-sepharose fast-flow column and then a phenyl-Sepharose column) of the recombinant proteins followed procedures described previously for recombinant *B. thuringiensis* PI-PLC (rPI-PLC) (*5*). The purity of PI-PLC enzymes was above 90% as monitored by SDS−PAGE. Protein solutions were concentrated using Millipore Centraplus 10 filters; concentrations were usually determined by Lowry assays (*11*), although absorption at 280 nm was also used.

CD Spectroscopy. Recombinant PI-PLC secondary structure was measured using an AVIV 202 CD spectrophotometer. Comparison of secondary structure for recombinant wild-type and mutated PI-PLC used wavelength scans from 265 to 195 nm with protein (0.3–0.4 mg/mL) in a 0.1 cm cell at 25 °C and the program CDNN (*12–14*).

^{31}P NMR Spectroscopy. The specific activity of PI-PLC mutant proteins was measured using ^{31}P NMR (202.3 MHz) spectra obtained on a Varian INOVA 500 using parameters described previously (*1, 5, 15*). Phosphorylated product formation for either fixed time points or continuous assays was analyzed (*7*). For both, the buffer was 25 mM HEPES, pH 7.5, and the amount of enzyme added in each kinetic run (50 ng to 3 μg depending on whether the phosphotransferase or the cyclic phosphodiesterase was monitored, respectively) was adjusted to generate less than 20% product within the desired reaction time. PI cleavage and cIP hydrolysis rates were measured from the integrated intensity of cIP and I-1-P resonances (in the absence of ^{1}H decoupling), respectively, as a function of incubation time, using the ^{31}P resonance of glucose 6-phosphate or KH_2PO_4 of known concentrations (2 or 4 mM) as an internal reference. The PI concentration was 5, 6, or 8 mM; diC$_7$PC was usually 24 or 32 mM but was also increased for surface dilution studies. The assay temperature was 28 °C. The hydrolysis of cIP (20 mM) was monitored in the absence or presence of 5 or 8 mM diC$_7$PC. For PI-PLC activity toward PI presented in small unilamellar vesicles (prepared by sonication), the PI concentration was 8 mM with 2 mM POPC. ^{31}P NMR was also used to monitor the interaction of two specific mutant proteins with the activator diC$_7$PC (*2, 8*). DiC$_7$PC was titrated into a solution of 3 mg/mL (0.085 mM) enzyme in 0.05 M HEPES and 1 mM EDTA, pH 7. In the presence of rPI-PLC, the line width of the diC$_7$PC phosphorus resonance was narrow below the CMC of that short-chain lipid, very broad around the CMC, and then narrowed as the concentration of diC$_7$PC increased further and the fraction of enzyme-bound diC$_7$PC decreased (*2, 8*). The magnitude of the line broadening reflects enzyme binding and diC$_7$PC dynamics and can be used to compare different PI-PLC mutant proteins. In an attempt to quantify the line broadening, we chose to extrapolate a "bound" line width for a 1:1 PI-PLC/diC$_7$PC complex by fitting the increased line width for diC$_7$PC [$\Delta\Delta\delta_{1/2} = \Delta v_{1/2}(+PLC) - \Delta v_{1/2}(PC)$] for lipid concentrations above the CMC of 1.5 mM with the following expression: $\Delta\Delta\delta_{1/2} = \Delta_b[PLC]/[diC_7PC] + \Delta v_{1/2}(limit)$, where Δ_b is the "bound" line width and $\Delta v_{1/2}(limit)$ is the increased diC$_7$PC line width caused by particle aggregation. This treatment, which assumes fast exchange for the diC$_7$PC in "empty" micelles, micelles containing PI-PLC, and monomeric diC$_7$PC, is simplistic but useful for assessing *differences* in mutated PI-PLC/diC$_7$PC interactions where specific activities are essentially the same.

Intrinsic Fluorescence of PI-PLC. Fluorescence measurements of PI-PLC (2 μM) were carried out on Shimadzu RF5000U or Fluorolog R-3 spectrofluorometers. The excitation wavelength was 282 nm. Changes in the fluorescence intensity at 337 nm (the emission maximum) upon the addition of lipids (either diC$_7$PC or POPC SUVs) were expressed as $(I - I_0)/I_0$, where I_0 is the emission intensity of protein alone and I is the intensity in the presence of an additive. An apparent binding constant to POPC vesicles was obtained by fitting the change in intensity with a hyperbolic function to extract a bulk concentration of PC for half the maximum change. For titrations with diC$_7$PC, the normalized change in fluorescence was fit with a cooperative function $[(I - I_0)/I_0 = \Delta I[PC]^n/(K_d^n + [PC]^n)]$, where ΔI was the maximum change in fluorescence and the apparent K_d for diC$_7$PC was the concentration of that lipid that led to half the maximum fluorescence change ($\Delta I/2$). The standard errors in K_d were derived from the least-squares fit of the concentration dependence of the fluorescence changes. To estimate an apparent K_d for "micellar" diC$_7$PC, only data above 1.5 mM were used, and the dependence of $(I - I_0)/I$ for diC$_7$PC concentrations above the CMC (1.5 mM) of pure lipid was plotted versus micellar diC$_7$PC (estimated as [PC] − CMC).

Centrifugation Vesicle Binding Assay. A centrifugation binding assay was used in addition to the fluorescence assay to characterize the binding of some PI-PLC mutants to interfaces (*6*). Solutions of PI-PLC incubated with phospholipid vesicles were centrifuged through a filter to separate free from vesicle-bound enzyme. Typically, 25 μg of PI-PLC (E_T) was added to an aliquot of the vesicle solution (2 mL) in 10 mM Tris-HCl, pH 7.5. Vesicle-bound enzyme (E_B) was separated from free enzyme (E_F) using an Amicon centricon-100 filter (100 kDa molecular mass cutoff). A control containing the same amount of enzyme in Tris-HCl, pH 7.5, with no lipid vesicles present indicated that less than 5% of E_T was retained on the filters in the control. Filtrates were lyophilized and analyzed by SDS−PAGE. Band intensities, quantified by NIH Image 1.61 software, were used to calculate the concentration of E_F by comparing intensities from vesicle-containing samples to the E_T value of the control; vesicle-bound enzyme, E_B, was calculated as $E_T - E_F$.

RESULTS

Helix B Alanine Mutations: Secondary Structure. A model (*9*) that has recently been proposed for the activation of *B. thuringiensis* PI-PLC upon binding to activating PC surfaces has the following steps. (i) In solution PI-PLC exists

primarily as a monomer, although small amounts of dimer have been noted previously (*8*). In the crystal structure of monomeric *B. cereus* PI-PLC (*4*), helix B points the hydrophobic side chains of Trp47 and Ile43 out into solution. (ii) The Trp47 in this hydrophobic plug sticking out from what appears to be a flexible helix B region is instrumental in protein binding to a PC surface. It should be noted that the protein has an electrostatic interaction with pure anionic lipids, but the binding does not involve insertion of the protein, and the protein can easily be removed from such a surface with moderate salt (*7*). The protein binds to the PC interface by inserting Trp47. (iii) Once bound to the PC surface, PI-PLC can form an interfacial homodimer using a string of Tyr residues (*9, 16*) near the barrel rim. It is the PLC dimer that is the kinetically activated form of the enzyme, presumably because it enhances processive catalysis and possibly alters some residues in and around the catalytic site leading to an increased k_{cat}. However, the only concrete evidence for PI-PLC dimer formation is from the crystal structure of W47A/W242A, a mutant with little affinity for PC surfaces.

While the crystallographic W47A/W242A dimer is unlikely to be the same as a membrane-bound PI-PLC dimer, it serves as a reference point for exploring residues that might be critical for dimerization. A key observation in the W47A/W242A dimer is that helix B no longer exists; rather the residues adopt a loop that is closer to the large rim loop that normally contains Trp242, another key Trp whose fluorescence intensity monitors membrane binding (*5*). Pro42, right before the start of helix B in the monomer crystal structure, contributes to dimer formation of W47A/W242A through hydrophobic interactions with both Tyr247 and Tyr248 of the opposite chain. In the dimer, Gln45 participates in a hydrogen bond with Gly239 of the opposite chain.

Since the dimer is of an interfacially impaired protein and residues in the helix B region appear to stabilize the dimer, there are two key questions: (i) Is the membrane-activated structure of this PI-PLC a dimer and (ii) is helix B intact when the protein binds to interfaces or does it form an extended loop as in W47A/W242A? Recent mutagenesis of a cluster of tyrosines (Tyr246, Tyr247, Tyr248, Tyr251) that form the hydrophobic core of the dimer interface in W47A/W242A strongly supports formation of a dimeric structure of PI-PLC on membranes as necessary for optimal activity (*16*). To assess the contribution of helix B to activity and binding of activator phospholipids, we have constructed alanine mutations at each position in helix B as well as at Leu39 and introduced a Gly in place of Pro42. All mutant genes overexpressed well in *E. coli* and generated proteins with similar CD spectra and T_m (as monitored by loss of negative ellipticity at 222 nm (*5*)) as rPI-PLC, indicating that the mutated proteins were well folded with the same overall structure. I43A, K44A, and W47A had the same secondary structure as rPI-PLC. However, L39A, P42G, Q45A, V46A, and G48A exhibited a reduced α-helix content (as much as 3% loss compared to the wild-type recombinant protein in solution) in low ionic strength buffers when compared by CD (Figure 3). For all of these but Q45A, the addition of 2 mM diC7PC caused the protein to regain α-helix structure to different degrees. These results illustrate a structural maleability in the helix B region of the protein when it is in solution.
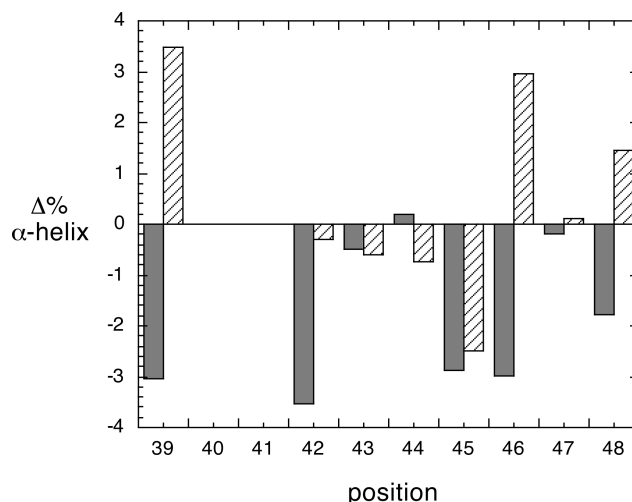

FIGURE 3: Difference in α-helix content for each mutant compared to recombinant PI-PLC protein (∼0.4 mg/mL in 10 mM borate buffer, pH 8.0, in 1 mm cuvette) in the absence (gray bars) and presence (hatched bars) of 2 mM diC7PC. For comparison, the secondary structure of the native protein from CD appears to be 25.5% α-helix, 24.4% β-sheet, 17.8% β-turn, and 32.3% random (*6*).

Phosphotransferase and Cyclic Phosphodiesterase Activities. If formation of a PI-PLC dimer is critical for high interfacial activity, then mutations in the helix B region that disrupt such a dimer should lead to reduced activity toward cIP in the presence of activating diC7PC (but not toward cIP alone). PI cleavage when presented in a PC surface might also be expected to decrease. A comparison of the cIP hydrolysis rates in the absence and presence of diC7PC is shown in Figure 4A for these helix B mutant enzymes. In the absence of any interfaces, all of the enzymes had cIP cleavage rates 58−96% of rPI-PLC enzyme activity (except for L39A and Q45A which exhibited 10% and 39% rPI-PLC activity). Thus, monomer substrate activity was more or less unaltered with this series of mutations. Addition of diC7PC micelles increased all cIP hydrolysis activities with the activation fold (ratio of the activity plus PC compared to that in its absence) comparable to rPI-PLC for L39A, I43A, and K44A; V46A was reasonably activated as well although not quite to the same extent (Figure 4B). P42G, Q45A, W47A, and G48A were all much less responsive to kinetic activation by this nonsubstrate phospholipid, suggesting either a reduction in diC7PC affinity or an altered conformation of the protein when bound to these micelles. The first two of these residues with lower PC activation of cIP hydrolysis are ones involved in dimer stabilization in W47A/W242A.

While the cyclic phosphodiesterase rates of P42G, Q45A, W47A, and G48A were very sensitive to modification of these helix B residues, the phosphotransferase activities only varied at most 3-fold (Figure 4C). Poor PC activation of cIP hydrolysis did not necessarily imply poor phosphotransferase activity (e.g., P42G and G48A show the opposite behavior). Conversely, for some enzymes with high cIP activation, phosphotransferase activity could be low (L39A, I43A). Since PI has acyl chains while cIP does not, these results hint that the presence of substrate with hydrophobic moieties can also lead to the "activated" conformation of PI-PLC.

Binding of Mutant Proteins to PC SUVs. In the model proposed, binding of PI-PLC to PC surfaces has two phases:
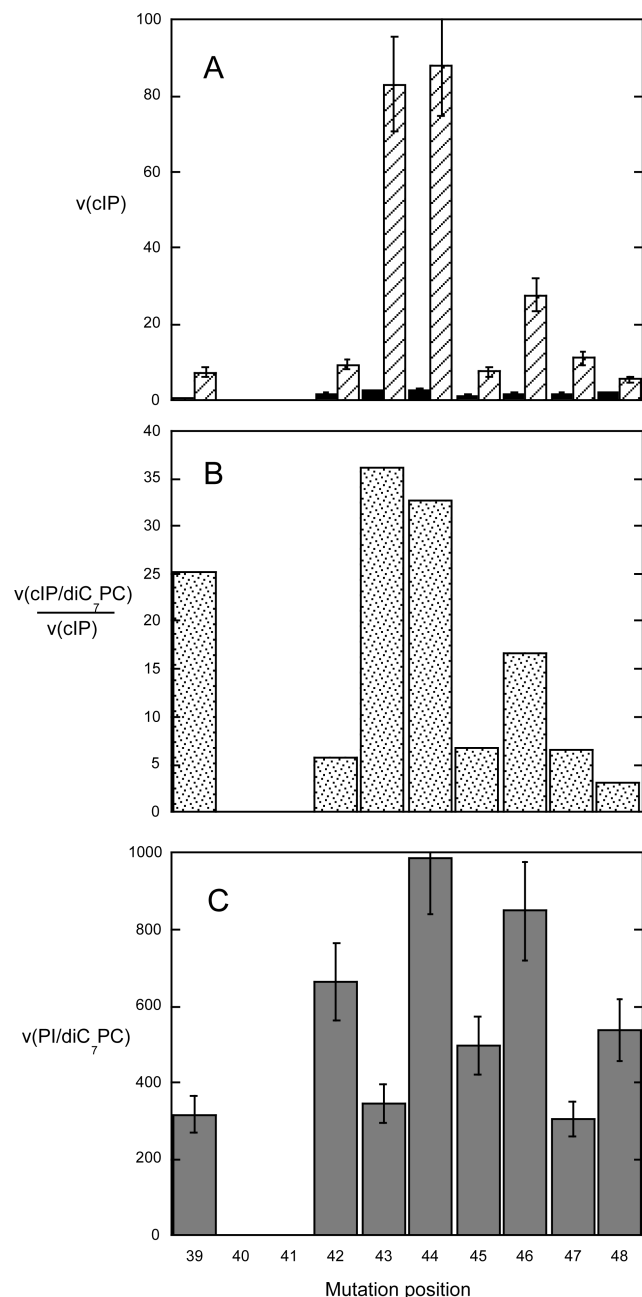
FIGURE 4: Activities (μmol min^{-1} mg^{-1}) of PI-PLC helix B region mutants with Ala or Gly (for P42G) substituted at the position indicated. (A) Specific activity for cleavage of 20 mM cIP in the absence (gray bars) and presence (hatched bars) of 8 mM diC$_7$PC. Error bars in (A) reflect standard deviations from multiple assays. (B) Extent of diC$_7$PC activation presented as the ratio of average cIP hydrolysis activity in the presence of diC$_7$PC compared to average activity in the absence of this nonsubstrate lipid. (C) Specific activity for cleavage of PI (8 mM) solubilized in 32 mM diC$_7$PC; error bars represent standard deviations for multiple assays.
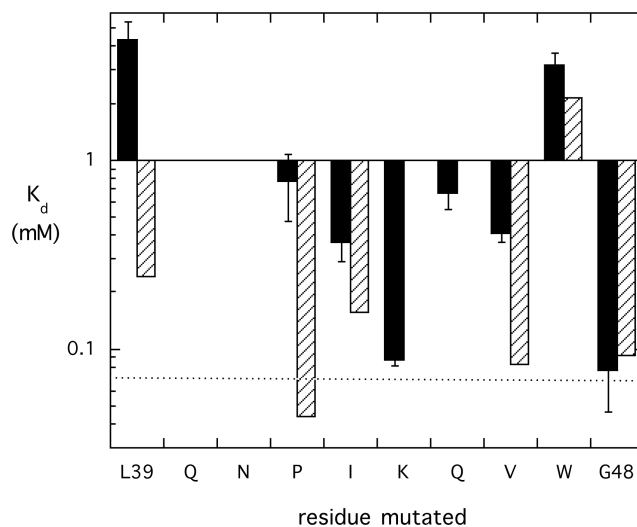

FIGURE 5: Apparent dissociation constants for helix B region mutants binding to POPC SUVs in 10 mM Tris-HCl, pH 7.5. The binding was monitored by both changes in the intrinsic Trp fluorescence as a function of added POPC SUVs and a filtration/centrifugation binding assay. The K_d in the hatched bars for the nonpolar side chains is what would be predicted for the K_d if that particular residue partitioned into the bilayer. The dashed line indicates the apparent K_d for wild-type recombinant PI-PLC.

binding, then interactions that destabilize the helix in solution would be expected to weaken binding of the protein to PC surfaces.

Recombinant PI-PLC bound moderately tightly to POPC SUVs with an apparent $K_d = 0.067 \pm 0.015$ mM (*6*). Of these helix B region mutant proteins, only K44A and G48A exhibited affinities for PC SUVs comparable to the rPI-PLC protein (Figure 5). Cationic Lys44 does not insert into membranes, and the structural change from Gly to Ala would not be expected to alter the K_d for G48A significantly. L39A and W47A had the weakest affinity for PC, with apparent K_d values roughly 50−70-fold more than that of rPI-PLC. The calculated K_d values for each protein in Figure 5 are based on free energy differences for side chains in membranes from the Wimley−White scale (*17*). The increased apparent K_d for W47A is clearly consistent with the indole ring partitioning into the membrane. However, the apparent K_d for the Leu39 substitution is far greater than expected solely on the basis of membrane partitioning. Although the Leu side chain could partition in the membrane, it is likely that substitution at this position also alters the protein conformation and disposition of other residues involved in membrane partitioning since the observed loss of binding affinity was so severe.

Alanine substitutions at the other positions in helix B exhibited a 6–12-fold loss of affinity for PC. Here, the loss of binding affinity does not correlate with changing the identity of a group that inserts into the membrane based on free energy changes. Rather, these residues must be involved in other interactions that modulate PC binding. In the crystal structure of *B. cereus* PI-PLC (*4*), helix B side chains do not interact significantly with the rest of the protein (Figure 2C,D). If helix B remains intact and acts as a hydrophobic plug for interface binding, only the removal of residues poised on the hydrophobic helix face, Ile43, Val46, and Trp47, should reduce membrane binding. However, in the W47A/W242A crystal dimer, both Pro42 and Gln45 make

an initial interaction and partitioning of Trp47 into the membrane (which presumably is achieved by monomeric protein) and then perhaps enhanced membrane binding once a homodimer is formed on the surface. If helix B need not be intact for initial binding to PC, then most of the mutant proteins would be expected to bind to PC, although affinities might be lower than rPI-PLC if dimerization does not occur to much extent. If helix B must be intact for the initial

Table 1: Relative Phosphotransferase (toward PI in Different Assay Systems) and Cyclic Phosphodiesterase (cIP as Substrate) Activities of rPI-PLC and Selected Helix B Mutants[a]

	5 mM PI in 30% iPrOH	5 mM PI in PI/diC$_7$PC (1:4)	5 mM PI in PI/TX100 (1:2)	8 mM PI in PI/POPC (4:1) SUVs	5 mM cIP[c] in diC$_7$PC (5 mM)	activation:[d] (+)diC$_7$PC/(−)diC$_7$PC
WT	0.72[b]	1.00	0.67[b]	0.017	0.19	46
I43A	0.32	0.36	0.31	0.006	0.15	36
I43W/W47A	0.13[b]	0.54[b]	0.42[b]	0.008	0.056	47
I43W/W47I	0.39	0.90	0.60	0.016	0.09	33
I43W	0.45	0.82	0.54	0.014	0.11	55
K44A	0.68	0.98	0.36	0.018	0.16	33
K44E		0.44			0.024	4.5

[a] All specific activities, except for K44E, were obtained at 22 °C and are referenced to cleavage of 5 mM PI solubilized in 20 mM diC$_7$PC (955 μmol min^{-1} mg^{-1} at 22 °C). Values are averages of fixed time point assays done in duplicate; errors were <15% of the indicated value. [b] From Feng et al. (5). [c] Values for cIP in the absence of activating PC were lower than reported previously (5, 7), which were obtained at a higher temperature (28 versus 22 °C). The value for rPI-PLC under these conditions was 2.8 μmol min^{-1} mg^{-1}. The ratio shown is for hydrolysis of 5 mM cIP in the presence of 5 mM diC$_7$PC. [d] The extent of PC activation of the enzyme for cIP hydrolysis was estimated by comparing specific activity in the presence of diC$_7$PC to the activity toward cIP alone.

Table 2: Apparent Binding Constants for Recombinant PI-PLC and Selected Helix B Mutants Interacting with PC Aggregates

	app K_d (mM) in POPC SUVs	calcd K_d (mM) in POPC SUVs	$K_{0.5}$ (mM)[a] in diC$_7$PC	$K_{0.5\text{-CMC}}$ (mM)[b] in micelles
WT	0.067 ± 0.010[c]		1.86 ± 0.08	0.36 ± 0.06
I43A	0.37 ± 0.07	0.15	2.28 ± 0.10	0.75 ± 0.06
I43W/W47A	0.85 ± 0.17[d]	0.15	2.48 ± 0.39[d]	1.08 ± 0.33[d]
I43W/W47I	0.064 ± 0.008	0.067	1.67 ± 0.07	0.18 ± 0.07
I43W	0.026 ± 0.06	0.005	1.65 ± 0.07	0.17 ± 0.09
K44A	0.087 ± 0.01		1.59 ± 0.07	0.08 ± 0.04
K44E	0.50 ± 0.20[e]			

[a] $K_{0.5}$ is estimated as the bulk concentration of diC$_7$PC that leads to 50% of the maximum change in fluorescence intensity upon binding to that short-chain PC; the value for WT PI-PLC is the average of three separate experiments. [b] $K_{0.5\text{-CMC}}$ is the value extracted for 50% of the fluorescence increase if only data above the CMC is used and fit with a hyperbolic function that reflects micellar diC$_7$PC only. Micellar PC is calculated as the concentration of diC$_7$PC minus the CMC (1.5 mM). [c] Extracted from data presented in ref 5. [d] Extracted from Feng et al. (7). [e] Estimated by using the increase in intrinsic florescence of the protein when it binds to PC vesicles (2, 13).

intersubunit contacts (Figure 2E,F). Therefore, the significantly weakened affinities of P42G and Q45A proteins (compared to rPI-PLC) for PC more likely reflect impaired dimerization on the membrane surface. Reduced dimerization could weaken the binding of the enzyme on the PC surface by increasing the off rate of the protein.

Positional and Charge Reversal Mutant Proteins of Helix B. If a helical hydrophobic plug (residues Ile43−Gly48) is needed for initial interaction of PI-PLC with PC, it should be stabilized by hydrophobic residues facing outward on the same side of helix B. Indeed, this is consistent with the observation that only I43W/W47A and no other Trp rescue mutation could significantly recover the PC interfacial activation of cIP hydrolysis lost in W47A (7). However, full PI cleavage activity was not observed with I43W/W47A, nor was it observed in I43A (Figure 4C). This might suggest that a specific positional arrangement of hydrophobic residues is critical in the helix B region of the protein. Two additional mutant proteins were examined to check for the importance of where the helix B Trp was placed. The "swap" mutation I43W/W47I should be equivalent to rPI-PLC kinetically and structurally if the actual position of Trp on helix B matters less than its orientation in solution and its stabilization by another hydrophobic side chain. I43W, which maintains the critical Trp47 residue in helix B (5), was made to see if the addition of a larger hydrophobic side chain had any effect on PI-PLC kinetic behavior. Both proteins had comparable secondary structure (data not shown) and similar phosphotransferase and cyclic phosphodiesterase specific activities (Table 1). Specific activities were determined for cleavage of PI solubilized in 30% iPrOH, PI in Triton X-100 micelles,

and PI in vesicles with 20 mol % PC as well as for the PI/diC$_7$PC mixed micelle system (Table 1). The "swap" mutant enzyme had similar activity to rPI-PLC in all but the iPrOH assay system (18, 19). I43W was not quite as active as rPI-PLC with the additional Trp residue in this region. Nonetheless, these results suggest that the position of the Trp in the helix B region is less important that its packing with another hydrophobic residue (presumably to stabilize helix B in solution).

I43W/W47I had about the same affinity for POPC SUVs as rPI-PLC (Table 2). I43A, where the Ile that stabilizes outward facing Trp47 in PI-PLC has been removed, had a weakened affinity for PC vesicles compared to rPI-PLC protein that correlates with its reduced phosphotransferase and PC activation of cIP hydrolysis rates. Changing Ile to Trp (I43W) enhanced enzyme partitioning to SUVs, but not enough to imply that both Trp in helix B are fully inserted into the PC membrane (the predicted K_d if both Trp insert would be 0.005 mM versus the experimental value of 0.026 mM).

We also examined in greater detail changes at residue 44. Lys44 represents the only charged residue in the helix B region. Replacement of the cationic side chain by a methyl group had no significant effect on enzyme activity in assay systems with PC or iPrOH or binding to PC vesicles (6). Specific phosphotransferase activity was only reduced with PI dispersed in Triton X-100. Clearly, removal of the cationic side chain in this region and replacement with a small neutral side chain do not contribute to enzyme binding to PC or to specific activity. However, replacing Lys44 with an anionic group (Glu) reverses the net charge on helix B and leads to
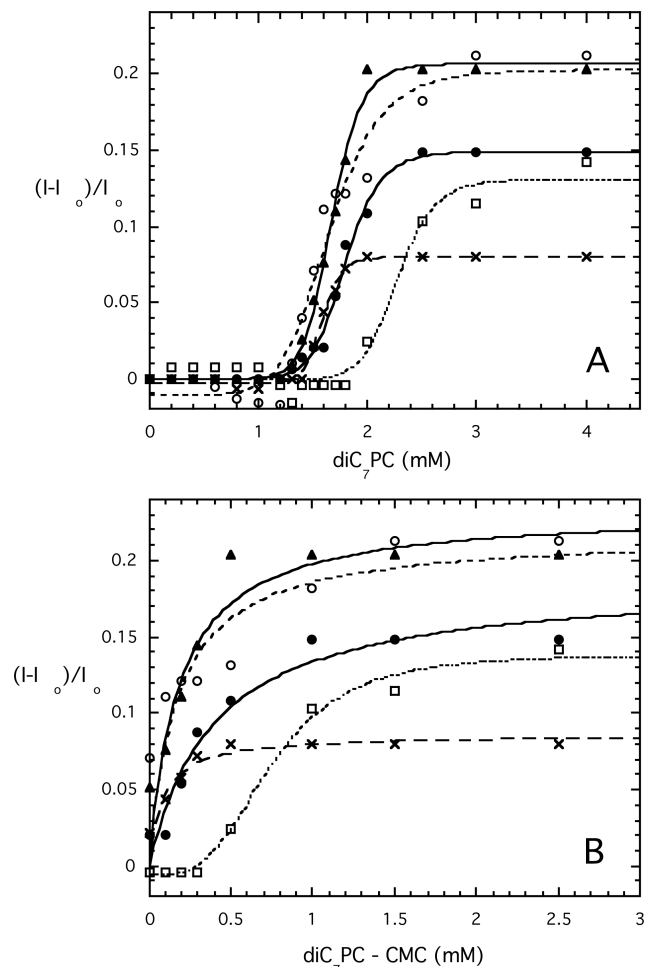
FIGURE 6: Increase in fluorescence intensities of *B. thuringiensis* PI-PLC proteins [WT (●), I43A (□), I43W (○), I43W/W47I (▲), K44A (×)] at 337 nm as a function of diC$_7$PC (A) total concentration and (B) micellar diC$_7$PC.

an enzyme, K44E, with both reduced PI cleavage and cIP hydrolysis in the presence of activating PC (Table 1) and reduced affinity for POPC vesicles (Table 2). Introduction of a negative charge at this position also weakens binding of the enzyme to PC interfaces. The K44E protein also had an unusual CD spectrum in that it had 7.4% less α-helix than rPI-PLC, suggesting less stable helical conformations in solution. However, the addition of 2 mM diC$_7$PC led to an increase in α-helix at the expense of β-sheet and random coil (similar to what was observed for P42G). The selective loss of PC activation, most noticeably for cIP hydrolysis, with the charge reversal of the lone charged group in helix B might suggest that it is very close to a PC binding site, possibly near the phosphate rather than the trimethylammonium moiety.

Previous work suggested that Trp242 is the main fluorophore responsible for the intrinsic fluorescence change when PI-PLC binds to activator PC micelles (*5*). As shown in Figure 6A, the change in fluorescence intensity of rPI-PLC upon micelle formation showed a steeper increase than that of I43A, consistent with the weaker binding of I43A to POPC surfaces. The mutant proteins I43W/W47I and I43W exhibited fluorescence behavior comparable to rPI-PLC. The $K_{0.5}$ values, which represent total diC$_7$PC, range from 1.59 to 2.48 mM. If the CMC for diC$_7$PC (1.5 mM) is subtracted from the bulk PC concentrations, and the resultant curves fit

(except for I43A) with a hyperbolic function (Figure 6B), we obtain apparent micelle K_d values that show a more striking change in micellar PC affinity (Table 2). Removal of the hydrophobic side chain of Ile43 or placing a Trp at this position and an Ala at 47 generates enzyme with weaker affinity for diC$_7$PC micelles. The sigmoidal nature of I43A strongly suggests that its binding is much weaker than the other mutated proteins examined since a higher amount of micellar diC$_7$PC must be present to observe binding (the sigmoidal behavior may result because the protein needs a certain concentration of micelles prior to binding rather than recruiting monomers to form a complex). The swapped mutant protein (I43W/W47I), I43W, and K44A all bind slightly more tightly to PC micelles than rPI-PLC protein (Table 2). Interestingly, K44A shows less than half the fluorescence change of rPI-PLC (Figure 6), indicating a difference in the environment of the dominant fluorophore, previously shown to be Trp242 (*5*), in this mutant protein. In monomeric PI-PLC structures (*4, 16*), residue 44 is not close to Trp242. However, in the W47A/W242A dimer, the residues in the helix B region are much closer to Trp242 in the rim loop (*9*).

PI-PLC-Induced Aggregation of diC$_7$PC. PI-PLC interaction with diC$_7$PC micelles can also be monitored by the increase in the ^{31}P line width of diC$_7$PC when the protein is present (*2*). The width at half-height, $\Delta v_{1/2}$, for the phosphorus resonance is broad in the presence of rPI-PLC protein as soon as the diC$_7$PC concentration is greater than the CMC (Figure 7). The very large increase in ^{31}P line width when recombinant wild-type protein binds to micellar diC$_7$PC reflects a combination of aggregation of the protein/diC$_7$PC system (*20*) and slower exchange between monomer, micelle, and enzyme-bound diC$_7$PC such that the exchange is intermediate on the NMR time scale (*2, 8*). At high concentrations of diC$_7$PC (~20 mM) where the ratio of diC$_7$PC/rPI-PLC is around 200, the limiting line width of the phosphorus in the presence of rPI-PLC is much larger than that for pure diC$_7$PC micelles. At 20 mM diC$_7$PC, if the diC$_7$PC molecules were in fast exchange between monomer, micelles of the same size as those in the absence of protein, and enzyme-sites, the weight-averaged line width should approach the line width of those pure diC$_7$PC micelles (~3 Hz). That it does not with rPI-PLC present is consistent with formation of an rPI-PLC/diC$_7$PC complex that is considerably larger than pure diC$_7$PC micelles and that likely alters the size distribution of diC$_7$PC micelles (*16*). Although the detailed contribution of different species and exchange rates to this observed line width has not been determined, the increased line width has been interpreted as formation of an activated PI-PLC aggregate (*20*). Interestingly, the same titration experiments carried out for I43W and I43W/W47I show much smaller increases in ^{31}P line width right above the CMC and much smaller limiting line widths (Figure 7). Both mutant proteins exhibit $K_{0.5}$ values for diC$_7$PC similar to rPI-PLC as measured by intrinsic fluorescence changes. From the difference in diC$_7$PC ^{31}P line widths in the absence and presence of protein at PC concentrations above the CMC, a "bound" line width, Δ_b (extrapolated broadening of one diC$_7$PC molecule caused by one PLC), can be estimated as well as an excess limiting particle line width, which must reflect increases in the average protein/lipid mixed micelle particle size. For rPI-PLC, $\Delta_b = 373 \pm 41$ Hz; this value is
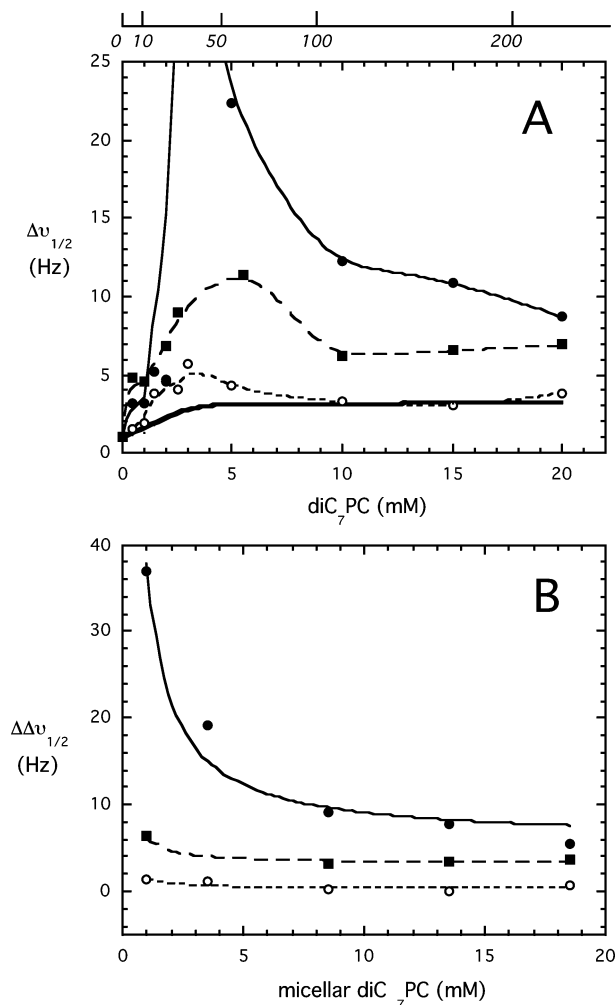
FIGURE 7: (A) ^{31}P line width (Hz) of the diC$_7$PC phosphorus resonance in the presence of 3 mg/mL WT (●), I43W (○), or I43W/W47I (■) PI-PLC. The top scale on the figure also shows the corresponding diC$_7$PC/PI-PLC ratio for these diC$_7$PC titrations. For comparison the line width for diC$_7$PC as a function of concentration without enzyme is shown (bold line). (B) Difference in diC$_7$PC line width ($\Delta\Delta\nu_{1/2}$) in the presence of PI-PLC for the three PI-PLC enzymes.

reduced to 36.1 ± 5.7 Hz for I43W/W47I and 14.1 ± 6.6 Hz for I43W. The limiting excess particle line width is 5.9 ± 1.6 Hz for rPI-PLC, 3.2 ± 0.2 Hz for the double mutant, and essentially zero (0.30 ± 0.27 Hz) for I43W. Since all three species are quite active, this suggests that the micellar aggregate structure per se is not responsible for diC$_7$PC activation of cIP hydrolysis. Rather the aggregation upon interaction with diC$_7$PC micelles is likely to reflect placement of the hydrophobic Trp residues at the rim of the PI-PLC barrel and the size and orientation of the hydrophobic plug this produces.

DISCUSSION

Interfacial activation of water-soluble phospholipases can occur by diverse mechanisms. In the case of the secreted bacterial PI-PLC from *Bacillus* sp., there is a very specific kinetic activation toward both phosphotransferase and phosphodiesterase substrates when a PC interface is present (*1–3, 21*). In the absence of PC and with moderate salt, the protein does not bind to vesicles composed of anionic phospholipids [e.g., phosphatidylmethanol (PMe), phosphatidylglycerol

(PG)] that are competitive inhibitors of PI (*3, 22*), while it binds well to PC vesicles. Enhanced PI cleavage in the presence of PC can then be explained by PC anchoring the protein to the interface, allowing it to access substrate. More problematic is how to explain activation (increased k_{cat} and decreased K_m) of diC$_4$PI cleavage or cIP hydrolysis (*1, 6*). Activation toward these monomeric substrates strongly indicates that binding to a PC surface alters the protein conformation to make it a better catalyst. However, determination of a detailed molecular picture of the mechanism for this activation has been difficult to achieve since the activation occurs on PC surfaces.

On the basis of the crystal structure of the monomeric *B. cereus* PI-PLC (*4*), the helix B region (Ile43 to Gly48) in wild-type PI-PLC, whose Trp residue has been proposed to partially insert into the membrane (*5, 7*), orients the side chains of Ile43 and Trp47 (and possibly Val46 as well) so that they pack together and form a hydrophobic protrusion that extends outward toward solvent. This would suggest that an intact helix B is critical for the initial interaction of PI-PLC with PC-containing membranes. However, a recent crystal structure (*9*) of an interfacially impaired mutant, W47A/W242A, showed that the helical secondary structure of the Ile43 to Gly48 segment has been disrupted to form an extended loop. The rim loop that would contain Trp242 has also been displaced. The removal of the two Trp residues thought to insert into membranes could explain the loss of PC binding and low phosphotransferase and cyclic phosphodiesterase activities. However, an unexpected and very interesting feature of this double mutation protein was that PI-PLC W47A/W242A exists in the crystal as a homodimer. Other crystal structures of this bacterial PI-PLC show that it is a monomer, and various sizing techniques showed the protein to have a predominantly monomer structure in solution (*2*). Residues in the helix B region, notably Pro42 and Gln45, play important roles in stabilizing the W47A/W242A dimer. The key question becomes whether a dimer forms with rPI-PLC on membrane surfaces and, if so, how close the structure of W47A/W242A is to the "active" dimer proposed to form on PC interfaces. Formation of a dimer on the membrane surface is appealing because it could provide the protein with an easier means of processive catalysis: release of water-soluble products by one subunit could occur with the other still tightly anchored to the membrane. Recent studies that examined mutations of three or more of the tyrosine residues that form the hydrophobic core of the dimer interface in W47A/W242A showed a dramatic loss of PI-PLC phosphotransferase and phosphodiesterase activities when these tyrosine residues, not close to the active site or directly around the barrel rim, were replaced with serine (*16*). Those results strongly support a dimer as the membrane-bound form of this PI-PLC. However, whether or not helix B is intact in the membrane-bound form still needs to be addressed.

The results in this study of mutating residues in the helix B region of PI-PLC are also consistent with dimer formation on PC interfaces. Q45A has reduced affinity for PC interfaces. Yet if helix B remains intact when the protein is bound to PC, the residue at position 45 could not contribute to membrane binding (or dimer formation) since it is on the opposite face of helix B (Figure 2D). With an intact helix B, both Ile43 and Trp47 would dominate binding of the helix
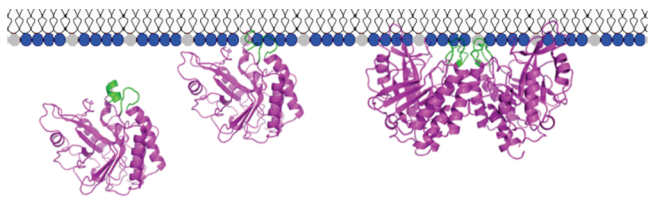
FIGURE 8: Model for the role of helix B residues in PI-PLC activation by PC interfaces.

to the membrane. The reduced PC activation of Q45A indicates that the membrane-active conformation of the enzyme is less favorable with this mutation, consistent with the hypothesis that helix B is unlikely to remain intact at the membrane surface during catalysis. In the W47A/W242A dimer Gln45 forms a hydrogen bond with Gly239 of the other subunit (Figure 2E). If this interaction contributes to rPI-PLC dimer stabilization of the membrane, Gln45 removal would be expected to disfavor dimer formation, thereby reducing PC affinity and enzyme activities. Indeed, both cIP and PI cleavage were reduced with the Q45A mutation. Pro42 is also involved in dimer stabilization in W47A/W242A. However, P42G could also alter helix B formation and orientation: the introduction of a very flexible residue allows the enzyme to have much greater variability in the helix B region. Interestingly, diC$_7$PC activation of cIP hydrolysis was reduced with only small effects on PI cleavage. If helix B in solution has been destabilized by introduction of a glycine at position 42, then the initial interaction of the protein with PC would be compromised. These results could also suggest that the presence of acyl chains on the bound PI substrate also contribute to dimerization of PI-PLC.

Leu39 provides an interesting wrinkle on membrane binding and dimer formation of *B. thuringiensis* PI-PLC. Like W47A, L39A binds very poorly to PC vesicles. Furthermore, the magnitude of the drop in affinity is much greater than would be predicted if an alanine rather than a leucine side chain partitioned in the membrane. In the crystal structure of *B. cereus* PI-PLC (4) as well as the W47A/W242A dimer (9), the side chain of Leu39 is embedded in the structure and would not be expected to have a significant effect on PC binding. The significantly weaker binding of L39A to POPC vesicles suggests the membrane-active dimer is not exactly the same as the W47A/W242A dimer and that there is a conformational change in this region of the barrel rim that either orients Leu39 outward so that it can partition directly into the PC surface and/or positions this residue to interact with the initial portions of the hydrophobic acyl chains of the substrate.

A proposed model for activation of *B. thuringiensis* PI-PLC is shown in Figure 8. PI-PLC in solution has an intact helix B (shown in green) that keeps the enzyme as a monomer and prevents premature dimerization (conformation A in Figure 8). Solution dimerization, were it to occur, might prevent tight binding of the protein to membranes since the resultant dimer (based on W47A/W242A) has a highly concave surface (9). An intact helix B also provides the hydrophobic surface for the initial binding of the protein to a PC membrane (or a PC-enriched region in mixed substrate/PC bilayers). Once contact occurs, Trp47 is inserted into the bilayer/interface. The insertion of Trp47 triggers a rearrangement of helix B residues altering both the position and

structure to an extended loop that could provide several points of contact, Ile43 and Val46 as well as Trp47, with the membrane (conformation B in Figure 8). Membrane-anchored protein monomers can now dimerize on the membrane surface via Tyr246, Tyr247, Tyr248, and Tyr251 residues (16) with both Pro42 and Gln45 part of the dimerization network. Enhanced PI cleavage to cIP would in part reflect the increased lifetime of the protein dimer on the membrane. However, other changes must occur for cIP hydrolysis to also be activated by PC interfaces. Work by us (1–3, 5–8, 21) and others (15, 20) has suggested that there is a conformational change in the *Bacillus* protein (as well as in a similar PI-PLC from *Listeria monocytogenes* (23)) when it binds to activating interfaces that increases k_{cat} and decreases the apparent K_d for membranes. This is reflected in a tighter affinity for activating interfaces (6, 8) and an increased inhibition of cIP hydrolysis by substrate analogues such as phosphatidic acid (PA) or PMe (21). In a W47A/W242A-like dimer, the accessibility of active site residues is altered to present a more extended surface (9) that should increase interactions of substrate molecules with the enzyme.

There are also likely to be more subtle changes in the active sites of the dimer that modulate the catalytic step. The transformation of PI to cIP occurs by His32 acting as a general base to deprotonate the inositol C(2)-OH so it can attack the phosphate group. His82 then acts as the general acid to protonate the DAG leaving group. In the second step (cIP hydrolysis to I-1-P), water, deprotonated by His82 acting as a general base, acts as a nucleophile to attack the phosphorus while protonated His32 contributes a proton to the inositol C2 oxygen. It has been suggested (24) that the catalytic triad of His82-Asp33-Arg69 is not optimally arranged to catalyze the hydrolysis of cIP. Rather, hydrophobic interactions of the rim and perhaps the hydrocarbon chains of the PI substrate facilitate the changes necessary for optimal catalysis (hence, PI cleavage will be much faster than cIP hydrolysis). For cIP in solution, both His32 and His82 would have the "wrong" initial ionization states. Enhancing catalysis, particularly for the second step, would be provided by an allosteric pathway between helix B residues and catalytic residues that shifts local pK_a values so that enhanced bond cleavage occurs. Binding to a PC interface provides this local change while not binding to the active site in place of cIP. Gly48, at the C-terminal end of helix B, would appear to be a key residue in this process. In structures of the *B. cereus* PI-PLC and W47A/W242A, Gly48 is close to His82 (<4 Å separation). While the binding of G48A to PC is very similar to rPI-PLC, the activities for both PI cleavage and cIP hydrolysis are lower than rPI-PLC. Furthermore, the activation by PC for cIP hydrolysis is dramatically decreased for this mutant enzyme relative to rPI-PLC (3-fold versus 22-fold activation). Since binding to PC induces a conformational change of the enzyme, Gly48 might be a very important site for communicating with the active site His82 about the conformational change of the helix B region.

REFERENCES

1. Zhou, C., Wu, Y., and Roberts, M. F. (1997) Activation of phosphatidylinositol-specific phospholipase C toward inositol 1,2-(cyclic)-phosphate. *Biochemistry 36*, 347–355.
2. Zhou, C., Qian, X., and Roberts, M. F. (1997) Allosteric activation of phosphatidylinositol-specific phospholipase C: specific phos-

pholipid binding anchors the enzyme to the interface. *Biochemistry 36*, 10089–10097.

3. Qian, X., Zhou, C., and Roberts, M. F. (1998) Phosphatidylcholine activation of bacterial phosphatidylinositol-specific phospholipase C toward PI vesicles. *Biochemistry 37*, 6513–6522.

4. Heinz, D. W., Ryan, M., Bullock, T. L., and Griffith, O. H. (1995) Crystal structure of the phosphatidylinositol-specific phospholipase C from Bacillus cereus in complex with myo-inositol. *EMBO J. 14*, 3855–3863.

5. Feng, J., Webhi, H., and Roberts, M. F. (2002) Role of tryptophan residues in interfacial binding of phosphatidylinositol-specific phospholipase C. *J. Biol. Chem. 277*, 19867–19875.

6. Wehbi, H., Feng, J., Kolbeck, J., Ananthanarayanan, B., Cho, W., and Roberts, M. F. (2003) Investigating the interfacial binding of bacterial phosphatidylinositol-specific phospholipase C. *Biochemistry 42*, 9374–9382.

7. Feng, J., Bradley, W., and Roberts, M. F. (2003) Optimizing the interfacial binding and activity of a bacterial phosphatidylinositol-specific phospholipase C. *J. Biol. Chem. 278*, 24651–24657.

8. Zhang, X., Wehbi, H., and Roberts, M. F. (2004) Cross-linking phosphatidylinositol-specific phospholipase C traps two activating phosphatidylcholine molecules on the enzyme. *J. Biol. Chem. 279*, 20490–20500.

9. Shao, C., Shi, X., Wehbi, H., Zambonelli, C., Head, J. F., Seaton, B. A., and Roberts, M. F. (2007) Dimer structure of an interfacially impaired phosphatidylinositol-specific phospholipase C. *J. Biol. Chem. 282*, 9228–9235.

10. Wang, W., and Malcolm, B. A. (1999) Two-stage PCR protocol allowing introduction of multiple mutations, deletions and insertions using QuikChange Site-Directed Mutagenesis. *BioTechniques 26*, 680–682.

11. Lowry, O. H., Rosebrough, N. J., Farr, A. L., and Randall, R. J. (1951) Protein measurement with the Folin phenol reagent. *J. Biol. Chem. 193*, 265–275.

12. Braman, J., Papworth, C., and Greener, A. (1996) Site-directed mutagenesis using double-stranded plasmid DNA templates. *Methods Mol. Biol. 57*, 31–44.

13. Bohm, G., Muhr, R., and Jaenicke, R. (1992) Quantitative analysis of protein far UV circular dichroism spectra by neural networks. *Protein Eng. 5*, 191–195.

14. Andrade, M. A., Chacon, P., Merelo, J. J., and Moran, F. (1993) Evaluation of secondary structure of proteins from UV circular dichroism spectra using an unsupervised learning neural network. *Protein Eng. 6*, 383–390.

15. Volwerk, J. J., Shashidhar, M. S., Kuppe, A., and Griffith, O. H. (1990) Phosphatidylinositol-specific phospholipase C from *Bacillus cereus* combines intrinsic phosphotransferase and cyclic phosphodiesterase activities: a ^{31}P NMR study. *Biochemistry 29*, 8056–8062.

16. Shi, X., Shao, C., Zhang, X., Zambonelli, C., Redfield, A. G., Head, J. F., Seaton, B. A., and Roberts, M. F. (2007) Modulation of *Bacillus thuringiensis* phosphatidylinositol-specific phospholipase C activity by mutations in the putative dimerization interface, J. Biol. Chem. (submitted for publication).

17. Wimley, W. C., and White, S. H. (1996) Experimentally determined hydrophobicity scale for proteins at membrane interfaces. *Nat. Struct. Biol. 3*, 842–848.

18. Wu, Y., and Roberts, M. F. (1997) Phosphatidylinositol-specific phospholipase C cyclic phosphodiesterase activity depends on solvent polarity. *Biochemistry 36*, 8514–8521.

19. Wehbi, H., Feng, J., and Roberts, M. F. (2003) Water-miscible organic cosolvents enhance phosphatidylinositol-specific phospholipase C phosphotransferase as well as phosphodiesterase activity. *Biochim. Biophys. Acta 1613*, 15–27.

20. Berg, O. G., Yu, B.-Z., Apitz-Castro, R. J., and Jain, M. K. (2004) Phosphatidylinositol-specific phospholipase C forms different complexes with monodisperse and micellar phosphatidylcholine. *Biochemistry 43*, 2080–2090.

21. Zhou, C., and Roberts, M. F. (1998) Nonessential activation and competitive inhibition of bacterial phosphatidylinositol-specific phospholipase C by short-chain phospholipids and analogues. *Biochemistry 37*, 16430–16439.

22. Roberts, M. F., and Redfield, A. G. (2004) High-resolution ^{31}P field cycling NMR as a probe of phospholipid dynamics. *J. Am. Chem. Soc. 126*, 13765–13777.

23. Ryan, M., Zaikova, T. O., Keana, J. F., Goldfine, H., and Griffith, O. H. (2002) *Listeria monocytogenes* phosphatidylinositol-specific phospholipase C: activation and allostery. *Biophys. Chem. 101–102*, 347–358.

24. Kubiak, R. J., Yue, X., Hondal, R. J., Mihai, C., Tsai, M. D., and Bruzik, K. S. (2001) Involvement of the Arg-Asp-His catalytic triad in enzymatic cleavage of the phosphodiester bond. *Biochemistry 40*, 5422–5432.